Horizontal Convection

Jennifer H. Siggers
University of Cambridge, U.K.

1 Introduction

The surface temperature of the ocean is different at different points. Can this differential heating drive a large scale flow? If so how large can that flow be? In this report we analyze a simple model of the ocean and construct rigorous upper bounds on the heat transport that can be induced by a horizontal temperature gradient that is imposed on the top surface. We consider the model shown in figure 1, where the top surface has an imposed temperature distribution with a cosine profile $\Delta T \cos kx + T_{\mathrm{av}}$, and make a linear transformation of the true temperature to give the new non-dimensional temperature variable T, which is equal to $\cos kx$ on the top boundary. This set up is known as horizontal convection [1]. Notice

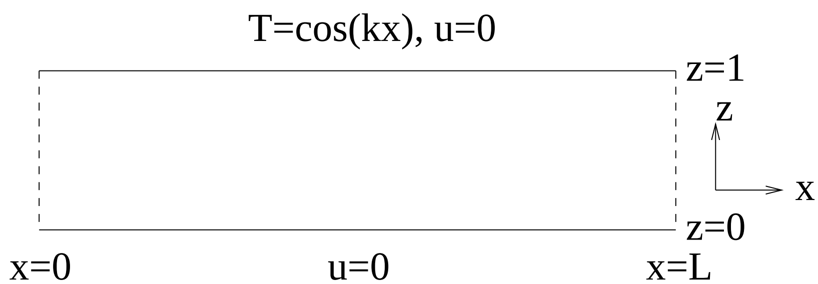

Figure 1: Set up of the horizontal convection problem

that the problem is in contrast to the usual Rayleigh–Bénard problem, where the motion is driven by vertical temperature gradients. In horizontal convection, it is the *horizontal* temperature gradient that drives the flow.

We use non-slip boundary conditions top and bottom and periodic side wall conditions, and we also need to specify a bottom boundary condition on the temperature. The box has dimensional width W and depth H and we non-dimensionalize these to give the new width $L = W/H$ and height 1. For horizontal periodicity, we also require that $k = 2\pi n/L$ for some $n \in \mathbb{N}$.

We aim to construct rigorous bounds on the total heat transfer rate through the layer, which we measure using a horizontal Nusselt number. We do this for variety of different temperature boundary conditions on the bottom of the layer to investigate the dependence of the scaling of the horizontal Nusselt number on the conditions there. This is because since horizontal convection is driven by temperatures at the top surface only, we want to find a bound that is independent of what is happening at the lower boundary. Also we don't have a good idea of what is the true oceanographic boundary condition there.

We use the Boussinesq approximation to reduce the equations to the standard non-

Quantity	Approximate value
ν	$1.52 \times 10^{-6} m^2 s^{-1}$
κ	$1.4 \times 10^{-7} m^2 s^{-1}$
$g\alpha\Delta T$	$10^{-2} m s^{-2}$
W	$2.0 \times 10^7 m$
H	$4 \times 10^3 m$
k	1.25×10^{-3}
R_H	3×10^{21}
σ	10.9
L	5.0×10^4

Figure 2: Approximate oceanographic values of some parameters, from [2]

dimensional form:

$$\dot{\mathbf{u}} + \mathbf{u} \cdot \boldsymbol{\nabla}\mathbf{u} + \boldsymbol{\nabla} p = \sigma R_H T \hat{\mathbf{z}} + \sigma \nabla^2 \mathbf{u}, \qquad (\mathcal{NS})$$

$$\dot{T} + \mathbf{u} \cdot \boldsymbol{\nabla} T = \nabla^2 T, \qquad (\mathcal{H})$$

$$\boldsymbol{\nabla} \cdot \mathbf{u} = 0, \qquad (\mathcal{C})$$

where $\mathbf{u}$ is the non-dimensional velocity field, T is the non-dimensional temperature and p is the non-dimensional pressure. $\sigma = \nu/\kappa$ is the Prandtl number and $R_H = H^3 g\alpha_T \Delta T/\kappa\nu$ is the horizontal Rayleigh number. ν is the kinematic viscosity, κ is the thermal diffusivity and g is the acceleration due to gravity. The table in figure 2 shows the approximate oceanographic values of some of these quantities. Note also that the governing equations do not possess a static solution, unlike the Rayleigh–Bénard problem, since from $(\mathcal{NS})$, we would need to satisfy $\boldsymbol{\nabla} p = \sigma R_H T \hat{\mathbf{z}}$. Since T must have some x-dependence in order to satisfy the boundary conditions, $T\hat{\mathbf{z}}$ cannot be gradient.

Thermal energy transport was considered by Sandström in the early 20th Century. He proposed the following theorem, (quoted from [3]):

> *Sandström's theorem*: "A closed steady circulation can only be maintained in the ocean if the heat source is situated at a lower level than the cold source."

This implies that horizontal convection cannot induce a large-scale flow and is therefore unimportant in the oceanic context. However, the theorem as it stands is not strictly true. For example, Jeffreys [4] constructed a counter example to Sandström's theorem, the "hula hoop" model, shown in figure 3. The fluid is contained in an annulus and heat is applied on the right hand side and the fluid is cooled on the left. Jeffreys argued that this heating and cooling will set the fluid in motion, no matter at what height the heating and cooling are applied, and thus we can heat near the top and cool near the bottom, as shown, and still induce a flow in the fluid. In some ways, this counter example is a bit contrived, but it is certainly a rigorous case where Sandström's theorem breaks down.

A second counter example is provided by Rossby [5], who performed some experiments on horizontal convection, using a set up similar to that in figure 1 except that he imposed the differential heating on the bottom surface and had insulating temperature boundary

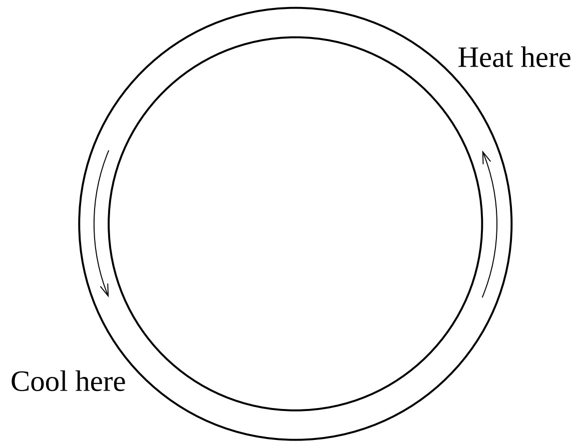

Figure 3: Schematic diagram of Jeffreys' hula hoop model

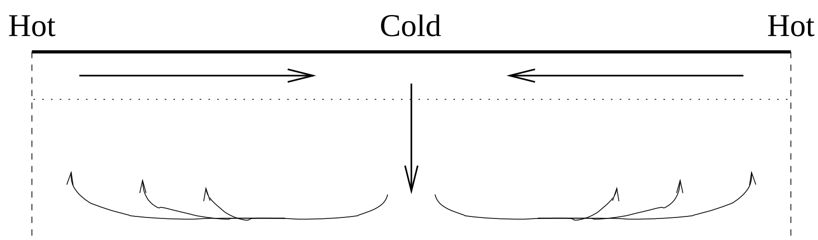

Figure 4: Schematic diagram showing the fluid motion. Note the strong downward motion in the central plume and large horizontal flows in the top boundary layer. There is also a slow recirculation in the rest of the layer.

conditions on the side and top walls. He found that there was a plume of hot rising water, over the hottest point on the bottom boundary. This rising motion induces a flow along the bottom of the box from the cold part to the hot part, and there is also a slow recirculation returning the fluid from the top of the box back down to the bottom.

However, even though Sandström's theorem is not completely true, in fact the main idea is correct: that thermal forcing at a single level as in the Rossby experiment is a relatively inefficient way to drive a flow when compared with Rayleigh–Bénard convection, for example, as we shall show in this report.

In the oceanic context the differential heating is at the top of the layer, which is why we consider this scenario rather than Rossby's though the two scenarios are linked via a reflection in the horizontal mid-plane, coupled with reversing the sign of the temperature field T. A schematic picture of the flow observed in numerical experiments (such as those in [6, 7, 8, 9]) is shown in figure 4, which is also the reverse of the flow that Rossby observed in his experiments. However, numerical simulations have only been performed for horizontal Rayleigh numbers R_H up to about 10^8, and it is not clear whether or not the flow structure in figure 4 persists into the oceanographic regime, in which $R_H \sim 10^{21}$.

Rossby [5] provided a consistent scaling argument for the width of the boundary layer in the flow. He assumed that there is a top boundary layer of width δ in which the vertical derivatives are of order δ^{-1} whilst the horizontal ones are of order unity. Then from $(\mathcal{H})$, balancing the advection term with the diffusion term, assuming temperature variations are of order 1 gives $\psi \sim \delta^{-1}$ and balancing the buoyancy term with the dissipation term in $(\mathcal{NS})$ yields $\delta \sim R_H^{-1/5}$.

Sandström [10] also proposed the following:

> *Sandström's conjecture*: "If a viscous and diffusive fluid is non-uniformly heated from above then in the limit $\kappa \to 0$ with $\sigma = \nu/\kappa$ fixed, the motion in the fluid disappears."

To make this rigorous quantitatively, we need a measure of the "motion in the fluid". Such a measure is the maximum value of the streamfunction. However, the conjecture as stated has not been proven. Instead we can prove a weaker result for horizontal convection in the form of an anti-turbulence theorem. We need to define a notion of turbulence, used by Frisch [11]:

> *The law of finite energy dissipation*: "If in an experiment on turbulent flow, all the control parameters are kept the same, except for the the viscosity, ν, which is lowered as much as possible, the energy dissipation per unit mass behaves in a way consistent with a finite positive limit."

This law is also known as the zeroth law of turbulence. In fact, this definition does not exclude non-laminar flows in a boundary layer, but it does give a precise definition to work with. Then we may propose

> *The anti-turbulence theorem*: If the only forcing is non-uniform heating applied at the surface of a Boussinesq fluid and if the viscosity, ν, and thermal diffusivity, κ are lowered to zero, with $\sigma = \nu/\kappa$ fixed, then in the limit the energy dissipation ϵ also vanishes.

This is finally a result that can be proved rigorously, which was done by Paparella and Young [9], who assumed a zero flux condition ($T_z = 0$) on the bottom boundary (where the subscript denotes differentiation with respect to z). It relies crucially on the following principle:

> *Boundedness principle for the temperature*: For the set up shown in figure 1, with an imposed temperature distribution on the top surface and a no flux bottom temperature boundary condition, then at any time the temperature field is bounded by the maximum and minimum values imposed on the top surface or the maximum and minimum values of the initial temperature distribution.

This can be proved from $(\mathcal{H})$. The derivation for a similar (but slightly more complicated) case is given in section 4.1. If the system is allowed to relax for a sufficiently long time, then we expect that the temperature is everywhere bounded by the maximum and minimum values at the top surface, that is, it lies in the range $[-1, +1]$.

We shall use an overbar to denote the horizontal and time average and angle brackets to denote the space and time average:

$$\overline{\cdot} = \lim_{t_0, y_0 \to \infty} \frac{1}{2t_0 y_0} \int_0^{t_0} \int_{-y_0}^{y_0} \int_0^L \cdot \, dx\, dy\, dt, \quad \langle \cdot \rangle = \int_0^1 \overline{\cdot}\, dz.$$

Now the energy dissipation per unit mass ϵ is given by $\nu\langle|\boldsymbol{\nabla}_d \mathbf{u}_d|^2\rangle$ where $\boldsymbol{\nabla}_d$ and $\mathbf{u}_d$ are the dimensional versions of $\boldsymbol{\nabla}$ and $\mathbf{u}$. In non-dimensional units, this becomes $\epsilon = \nu\kappa^2\langle|\boldsymbol{\nabla}\mathbf{u}|^2\rangle/H^4$, and rearranging $\langle \mathbf{u}\cdot(\mathcal{NS})\rangle$ we have

$$\epsilon = \frac{\nu\kappa^2 R_H}{H^4}\langle wT\rangle.$$

Taking $\langle(1-z)\cdot(\mathcal{H})\rangle$ gives $\langle wT\rangle = -\overline{T}|_0$ and so

$$\epsilon = \frac{\nu\kappa^2 R_H}{H^4}\left(-\overline{T}|_0\right) \leq \frac{\nu\kappa^2 R_H}{H^4} = \frac{\kappa g\alpha\Delta T}{H} \to 0 \quad \text{as } \kappa \to 0,$$

where the inequality makes use of the lower bound on the temperature field, thus proving anti-turbulence.

In this report, we try to construct bounds on the strength of the convection for horizontal convection. Often the Nusselt number is used as a measure of the strength, but this measures the heat flux in the *vertical* direction, whereas for horizontal convection it is the *horizontal* heat flux that is of interest. Thus we need to define a horizontal Nusselt number Nu_H. Ideally this would measure the total heat flux into (or equivalently out of) the top boundary, i.e.

$$\overline{\chi(x,y,t)T_z(x,y,1,t)},$$

where $\chi(x,y,t)$ equals 1 if $T_z(x,y,1,t) > 0$ (corresponding to places where there is flux in) and 0 otherwise (corresponding to flux out). With a zero flux bottom boundary condition this equals $\overline{|T_z|}|_1/2$. However, we don't know which parts of the top boundary have heat fluxes into the layer and which have fluxes out and thus we don't know χ. We might assume a symmetric arrangement, in which if $T > 0$ at the top of the layer then there is a heat flux out of the layer (i.e. $T_z < 0$), and if $T < 0$ then the heat flux is into the layer (i.e. $T_z > 0$). However, the solutions found in the numerics (see figure 4) are far from symmetric due to the cold plume, and so we might expect the area of the top surface where χ is 1 to be confined to a small areas around the points where T takes its maximum value. Thus, this definition of the horizontal Nusselt number would be extremely hard to estimate mathematically, and instead we propose an alternative formulation.

In [9], which considered a zero flux bottom boundary condition, the form

$$Nu_H = \frac{\langle|\boldsymbol{\nabla}T|^2\rangle}{\langle|\boldsymbol{\nabla}T_c|^2\rangle}, \tag{1}$$

was used, where, since there is no static solution of the equations, we define the "conduction" solution T_c to be the steady solution of the horizontal convection problem where the fluid is replaced by a solid (and thus we can neglect $(\mathcal{NS})$ and just solve $(\mathcal{H})$ with $\mathbf{u} = 0$), so T_c is the solution of $\nabla^2 T_c = 0$ together with the boundary conditions on T. The justification for the formula (1) can be seen if we take the time average of $(\mathcal{H})$, integrate over the vertical coordinate and take the average over the y-coordinate:

$$\lim_{t_0\to\infty, y_0\to\infty} \frac{1}{2t_0y_0}\int_0^{t_0}\int_{-y_0}^{y_0}\int_0^1 \left((uT)_x - T_{xx}\right) dzdydt$$
$$= \lim_{t_0\to\infty, y_0\to\infty} \frac{1}{2t_0y_0}\int_0^{t_0}\int_{-y_0}^{y_0} \left(T_z|_1 - T_z|_0\right) dydt.$$

Integrating with respect to x gives

$$J_H(x) := \lim_{t_0\to\infty, y_0\to\infty} \frac{1}{2t_0 y_0} \int_0^{t_0} \int_{-y_0}^{y_0} \int_0^1 (uT - T_x)\, dz dy dt$$
$$= \lim_{t_0\to\infty, y_0\to\infty} \frac{1}{2t_0 y_0} \int_0^{t_0} \int_{-y_0}^{y_0} \int^x (T_z|_1 - T_z|_0)\, dx' dy dt.$$

J_H is the average heat flux through a plane of constant x, which, in general, is not constant as x varies, so to obtain a formula for the horizontal Nusselt number, we must take a weighted average over x of the form $\overline{f(x)J_H(x)}$. Looking at the form of the flow in figure 4, we want f to be positive in the left half (where the heat transport is expected to be in the $+x$ direction) and negative in the right half. A simple weighting function f satisfying these requirements is $-dT(x,y,1,t)/dx = k\sin kx$. Taking the average and integrating by parts gives

$$\overline{k\sin kx J_H} = \overline{\cos kx T_z}|_1 - \overline{\cos kx T_z}|_0, \tag{2}$$

which equals $\overline{\cos kx T_z}|_1$ with the zero flux bottom boundary condition. The horizontal Nusselt number is this quantity normalized by the corresponding value for the "conduction" state. Rearranging $\langle T\cdot(\mathcal{H})\rangle$ gives

$$\langle|\boldsymbol{\nabla} T|^2\rangle = \overline{\cos kx T_z}|_1 - \overline{TT_z}|_0, \tag{3}$$

and for a zero flux bottom temperature boundary condition, $\overline{TT_z}|_0$ vanishes, meaning that we obtain the form (1).

If instead we have a different bottom boundary condition for which the second equality in (2) does not hold identically (such as fixed temperature there) then the term $\overline{\cos kx T_z}|_0$ is too difficult to estimate mathematically and so since we expect the fluxes through the top boundary to be much larger than those through the bottom, we neglect this term and in general we define the horizontal Nusselt number to be

$$Nu_H = \frac{\overline{\cos kx T_z}|_1}{\overline{\cos kx T_{cz}}|_1} = \frac{\langle|\boldsymbol{\nabla} T|^2\rangle + \overline{TT_z}|_0}{\overline{\cos kx T_{cz}}|_1}, \tag{4}$$

where the second equality is derived from (3).

In this report, rigorous bounds on the horizontal Nusselt number, as defined by (4), will be sought for the problem of horizontal convection with the set up shown in figure 1, using a variety of different bottom boundary conditions for the temperature. In section 2 we impose a fixed flux condition, and in section 3 a fixed temperature boundary condition. We obtain different scalings for the two cases and since the ocean floor is neither a perfect conductor nor a perfect insulator, in section 4 we use a boundary condition that can smoothly move between fixed flux and fixed temperature, and investigate how the scalings change as we move away from these two limits.

2 Fixed Flux Bottom Boundary Condition

We consider the horizontal convection set up shown in figure 1 with fixed positive heat flux $T_z = -F$ at the bottom of the layer. With this set up, the "conduction" solution T_c is given by

$$T_c = \frac{\cosh kz}{\cosh k}\cos kx + F(1-z).$$

Then the denominator of the horizontal Nusselt number (4) is

$$\overline{\cos kx T_{cz}}|_1 = \frac{k}{2}\tanh k.$$

If $F > 0$, corresponding to a heat flux into the layer, then the temperature field is bounded from below for all time by the minimum of -1 and $\inf(T|_{t=0})$. Assuming that we have left the system to relax for long enough, then $T \geq -1$ everywhere. However, with this particular boundary condition, there is no analogous upper bound on the temperature field.

2.1 Bound on the Horizontal Nusselt Number Using the Lower Bound on the Temperature

We try to find the maximum value of the horizontal Nusselt number by using the Doering–Constantin background method [12]. We let $T(\mathbf{x}, t) = \tau(x, z) + \theta(\mathbf{x}, t)$, where the background field τ satisfies the boundary conditions on T and therefore θ satisfies the homogeneous boundary conditions ($\theta = 0$ at $z = 1$ and $\theta_z = 0$ at $z = 0$). Note that in contrast to [12], in which τ is a function of z only, here τ must depend on the horizontal coordinate in order to satisfy the boundary conditions. We consider the variational formulation to bound the numerator of (4):

$$\mathcal{L} = \overline{\cos kx T_z}|_1 - a\langle \mathbf{u}\cdot(\mathcal{NS})\rangle - b\langle \theta\cdot(\mathcal{H})\rangle,$$

where a and b are constant Lagrange multipliers. The first term in this expression is the term we are trying to bound and from this we subtract the constraints we wish to satisfy, multiplied by the Lagrange multipliers a and b. Ideally we would require the full equations ($\mathcal{NS}$,$\mathcal{H}$,$\mathcal{C}$) to be satisfied at every point in the domain for all times, but this is too complicated to do analytically. Rearranging gives

$$\mathcal{L} = \left\langle |\boldsymbol{\nabla}\tau|^2 - a\sigma|\boldsymbol{\nabla}\mathbf{u}|^2 - (b-1)|\boldsymbol{\nabla}\theta|^2 + (b-2)\theta\nabla^2\tau - b\theta\mathbf{u}\cdot\boldsymbol{\nabla}\tau \right\rangle + a\sigma R_H\langle wT\rangle - F\overline{T}|_0 + 2F\overline{\theta}|_0, \quad (5)$$

and by taking $\langle(1-z)\cdot(\mathcal{H})\rangle$, we get $\langle wT\rangle = F - \overline{T}|_0$. Using the fact that, as long as $F \geq 0$, the temperature field is bounded from below by -1, and assuming that $a\sigma R_H - F \geq 0$ (to be checked a posteriori), we can bound the final three terms:

$$a\sigma R_H\langle wT\rangle - F\overline{T}|_0 + 2F\overline{\theta}|_0 = a\sigma R_H F - (a\sigma R_H - F)\overline{T}|_0 - 2F\overline{\tau}|_0 \leq a\sigma R_H(F+1) - F - 2F\overline{\tau}|_0.$$

All the terms in this expression are either independent of θ and $\mathbf{u}$, or depend linearly on these quantities or are quadratic negative semi-definite terms, except for the term $\langle -b\theta\mathbf{u}\cdot\boldsymbol{\nabla}\tau\rangle$. If this term is removed the whole expression is bounded above, and straightforward to maximize. Thus we first bound this this term by quadratic semi-definite quantities and then find and solve the Euler–Lagrange equations for the resulting functional to obtain a bound.

Our choice of background field τ is designed to minimize the worst case estimate of $\langle -b\theta\mathbf{u}\cdot\boldsymbol{\nabla}\tau\rangle$. We should ideally like to set $\boldsymbol{\nabla}\tau = 0$ everywhere, but then we cannot satisfy the boundary conditions. Instead we choose $\boldsymbol{\nabla}\tau = 0$ everywhere except for a boundary layer top and bottom. We set $\tau = \tau_0(z) + \tau_1(z)\cos kx$ where

$$\tau_0 = \begin{cases} F(\delta_0 - z), & \text{for } 0 < z < \delta_0, \\ 0, & \text{for } \delta_0 < z < 1, \end{cases} \tag{6}$$

$$\tau_1 = \begin{cases} 0, & \text{for } 0 < z < 1 - \delta_1, \\ \frac{z-1+\delta_1}{\delta_1}, & \text{for } 1 - \delta_1 < z < 1, \end{cases} \tag{7}$$

Now we can estimate $\langle -b\theta\mathbf{u}\cdot\boldsymbol{\nabla}\tau\rangle$. This only has contributions from the top and bottom boundary layers, and using the estimates (27), (28) and (30) in appendix A, we obtain

$$\langle -b\theta\mathbf{u}\cdot\boldsymbol{\nabla}\tau\rangle \leq \alpha\langle|\boldsymbol{\nabla}\mathbf{u}|^2\rangle + \beta\langle|\boldsymbol{\nabla}\theta|^2\rangle,$$

where

$$\alpha = b\max\left(\frac{F\delta_0^2 c_0}{2\pi^2}, \frac{\delta_1 c_1}{2\pi^2}(1+2k\delta_1)\right),$$
$$\beta = b\left(\frac{F\delta_0}{2c_0} + \frac{2\delta_1}{\pi^2 c_1}(1+2k\delta_1)\right).$$

So

$$\mathcal{L} \leq \langle|\boldsymbol{\nabla}\tau|^2 - (a\sigma-\alpha)|\boldsymbol{\nabla}\mathbf{u}|^2 - (b-1-\beta)|\boldsymbol{\nabla}\theta|^2 + (b-2)\theta\nabla^2\tau\rangle + a\sigma R_H(1+F) - F(1+2F\delta_0).$$

The Euler–Lagrange equations for an extremal value of the functional are

$$\boldsymbol{\nabla}p - 2(a\sigma-\alpha)\nabla^2\mathbf{u} = 0, \tag{8}$$
$$-2(b-1-\beta)\nabla^2\theta = (b-2)\nabla^2\tau, \tag{9}$$

where the term $\boldsymbol{\nabla}p$ has been added to ensure incompressibility, yielding the solution

$$\theta^* = \frac{-(b-2)}{2(b-1-\beta)}(\tau - T_c), \quad \mathbf{u}^* = 0,$$

which maximizes the functional as long as the spectral constraints $a\sigma \geq \alpha$ and $b-1 \geq \beta$ are satisfied. Substituting in the expressions for the extremalizing fields $\mathbf{u}^*$ and θ^*, we get a bound on $\mathcal{L}$. Dotting (9) by θ^* and averaging, we obtain an equation that allows us to simplify the bound, giving

$$\mathcal{L} \leq \langle|\boldsymbol{\nabla}\tau|^2\rangle + \frac{(b-2)^2}{4(b-1-\beta)}\left(\langle\boldsymbol{\nabla}\tau\cdot\boldsymbol{\nabla}(\tau-T_c)\rangle - F\overline{(\tau-T_c)}|_0\right) + a\sigma R_H(1+F) - F(1+2F\delta_0).$$

For our choice of τ,

$$\langle|\boldsymbol{\nabla}\tau|^2\rangle = F^2\delta_0 + \frac{1}{2\delta_1} + \frac{k^2\delta_1}{6},$$
$$\langle\nabla\tau\cdot\nabla T_c\rangle = F^2\delta_0 + \frac{k}{2}\tanh k,$$

meaning that

$$\mathcal{L} \le \frac{1}{2\delta_1} + \frac{k^2\delta_1}{6} + \frac{(b-2)^2}{4(b-1-\beta)}\left(\frac{1}{2\delta_1} + \frac{k^2\delta_1}{6} - \frac{k}{2}\tanh k + F^2(1-\delta_0)\right) + a\sigma R_H(1+F) - F - \delta_0 F^2. \quad (10)$$

To obtain the tightest bound we need to minimize (10) subject to the spectral constraints. These are of the form

$$a\sigma \ge b\max(Pc_0, Qc_1), \quad b-1 \ge b\left(\frac{R}{c_0} + \frac{S}{c_1}\right),$$

where P, Q, R and S are independent of a, b, c_0 and c_1. Thus they are satisfied if and only if

$$\frac{a\sigma(b-1)}{b^2}\lambda \ge PR + PS\frac{c_0}{c_1}, \quad \frac{a\sigma(b-1)}{b^2} \ge QR\frac{c_1}{c_0} + QS.$$

A suitable value of c_0/c_1 can be chosen if and only if

$$\frac{a\sigma(b-1)}{b^2}\left(\frac{a\sigma(b-1)}{b^2} - PR - QS\right) \ge 0,$$

and since $a\sigma(b-1)/b^2 \ge 0$, the spectral constraints are equivalent to $a\sigma \ge (PR+QS)b^2/(b-1)$.

Since both $b^2/(b-1)$ and $(b-2)^2/4(b-1-\beta)$ are minimized at $b=2$ (and the quantity in the bracket multiplying $(b-2)^2/4(b-1-\beta)$ in (10) is positive) this means that $b=2$ is optimal in that it minimizes the right hand side of (10). We should also minimize $a\sigma$, so we set

$$a\sigma = \left(\frac{F^2\delta_0^3}{\pi^2} + \frac{4\delta_1^2}{\pi^4}(1+2k\delta_1)^2\right).$$

For sufficiently large Rayleigh numbers, the value of δ_0 is insignificant at leading order but we want δ_1 to be as large as possible and so we set $\delta_0 = 0$ and $a\sigma = 4\delta_1^2(1+2k\delta_1)^2/\pi^4$, leaving us with

$$\mathcal{L} \le \frac{1}{2\delta_1} + \frac{k^2\delta_1}{6} + \frac{4\delta_1^2}{\pi^4}(1+2k\delta_1)^2 R_H(1+F) - F.$$

For sufficiently large R_H, the leading order terms will be $1/2\delta_1 + 4\delta_1^2 R_H(1+F)/\pi^4$. These are minimized with the choice $\delta_1 = (\pi/2)^{4/3}(R_H(1+F))^{-1/3}$, yielding the leading order bound $\mathcal{L} \lesssim 3(R_H(1+F))^{1/3}/2^{2/3}\pi^{4/3}$ and so

$$\boxed{Nu_H \lesssim \frac{3\cdot 2^{1/3}(1+F)^{1/3}}{\pi^{4/3}k\tanh k}R_H^{1/3},} \quad (11)$$

to leading order.

Note that we assumed $a\sigma R_H - F \ge 0$, which is always true for the given scalings as $R_H \to \infty$ with F fixed. However, if F is very large (i.e. if $F^3(1+F)^2 \ge (1+2k\delta_1)^6 R_H/4\pi^4$)

we cannot use the lower bound on T. We could choose $a\sigma R_H - F = 0$ yielding the leading order bound

$$Nu_H \lesssim \left(\frac{1}{\pi^2}\sqrt{\frac{R_H}{F}} + F^2 \right) \bigg/ \frac{1}{2} k \tanh k, \tag{12}$$

if $R_H^{1/5} \lesssim F \lesssim R_H$ and

$$Nu_H \lesssim \frac{2F^2}{k \tanh k}, \tag{13}$$

if $F \gtrsim R_H$. However, this is probably not optimal since we have been forced to choose $a\sigma R_H - F \geq 0$ in order to use the fact that $T \geq -1$ everywhere. For $F \gg 0$, we might expect that T is well above -1 at the bottom boundary. Instead in the next section we bound the horizontal Nusselt number without using the bound on the temperature to see if we can get a better bound for Nu_H when F is large.

2.2 Bound on the Horizontal Nusselt Number Without Using the Lower Bound on the Temperature

As F becomes larger, since there are steep negative temperature gradients at the bottom boundary, we expect that the lower bound on the temperature there gives a poor estimate of the actual temperature. To attempt to find a better scaling, we do not use this lower bound and instead we must find an alternative way to bound the final three terms in (5). We have

$$a\sigma R_H \langle wT \rangle - F\overline{T}|_0 + 2F\overline{\theta}|_0 = (a\sigma R_H - F)\langle w(\tau + \theta) \rangle + F^2 - 2F\overline{\tau}|_0,$$

and now the sign-indeterminate quadratic terms contributing to $\mathcal{L}$ are

$$\langle (a\sigma R_H - F) w\theta - b\theta \mathbf{u} \cdot \boldsymbol{\nabla}\tau \rangle,$$

which we bound by $\alpha\langle|\boldsymbol{\nabla}\mathbf{u}|^2\rangle + \beta\langle|\boldsymbol{\nabla}\theta|^2\rangle$ for suitable α and β. We choose the background field τ so that the integrand is zero over as much of the layer as possible. To do this we use $\tau = \tau_0(z) + \tau_1(z)\cos kx$ where τ_1 is again given by (7) and

$$\tau_0 = \begin{cases} F(\delta_0 - z) - \frac{(a\sigma R_H - F)}{b}(1 - \delta_0), & \text{for } 0 < z < \delta_0, \\ -\frac{(a\sigma R_H - F)}{b}(1 - z), & \text{for } \delta_0 < z < 1, \end{cases}$$

which means that the integrand is zero everywhere except in the boundary layers, and estimate α and β using the bounds in appendix A.

Proceeding in the same way as for the small F case, we obtain the Euler–Lagrange equations

$$\boldsymbol{\nabla} p - 2(a\sigma - \alpha)\nabla^2 \mathbf{u} = (a\sigma R_H - F)\tau\hat{\mathbf{z}},$$
$$-2(b - 1 - \beta)\nabla^2\theta = (b - 2)\nabla^2\tau,$$

which have the same solution for θ, but now the solution for $\mathbf{u}$ is non-zero. Substituting in the extremal values $\mathbf{u}^*$ and θ^* gives

$$\mathcal{L} \leq \langle|\boldsymbol{\nabla}\tau|^2\rangle + \frac{(b-2)^2}{4(b-1-\beta)}\left(\langle\boldsymbol{\nabla}\tau\cdot\boldsymbol{\nabla}(\tau-T_c)\rangle - F\overline{(\tau-T_c)|_0}\right) + \frac{1}{2}(a\sigma R_H - F)\langle w^*\tau\rangle$$
$$+ F^2 - 2F\left(F\delta_0 - \frac{a\sigma R_H - F}{b}(1-\delta_0)\right).$$

$\langle w^*\tau\rangle$ is estimated in equation (34) in appendix B, and we proceed in the same way as for small F. The best choice at leading order for $R_H \to \infty$ is $\delta_0 = 0$, $a\sigma = 4\delta_1^2/\pi^4$, $\delta_1 = \pi^{8/5}/2^{1/5}\cdot 3^{2/5}R_H^{2/5}$ and $b = 8/3$ and we get

$$\boxed{Nu_H \lesssim \frac{2^{11/5}R_H^{2/5}}{3^{3/5}\pi^{8/5}k\tanh k}.} \tag{14}$$

and so this bound is not as good as (11). However, when $F \gg R_H^{1/5}$ we can show that $Nu_H \lesssim (3b^3 - 8b^2 + b + 8)F^2/2b(b-1)k\tanh k$ at leading order. This bound is minimized when $b \approx 1.87$, giving

$$Nu_H \lesssim \frac{0.46F^2}{k\tanh k},$$

thus improving the *prefactor* of the corresponding results (12) and (13) in the previous section, but not the order of magnitude of the bound.

2.3 Application to the Real Ocean!

The total heat flux from the Earth's interior is $F_E = 3\times 10^{13}W$. For a large ocean, such as the Pacific or Atlantic, this means that the non-dimensional flux on the ocean floor is

$$F = \frac{F_E H}{c\rho A\kappa\Delta T} \approx 60,$$

where $H \sim 4000m$, $c = 4184Jkg^{-1}K^{-1}$ is the specific heat of the water, $\rho = 1000kgm^{-3}$ is the density, $A = 4\pi(6.4\times 10^6)^2m^2$ is the area of the surface of the Earth. Thus the $R_H^{1/3}$ scaling is appropriate here and with $k \sim 1.25\times 10^{-3}$ we obtain $Nu_H \lesssim 10^{13}$. The dimensionalized heat flux in an ocean covering the whole Earth would be approximately

$$\frac{c\rho A\kappa\Delta T}{H}\overline{\sin kxJ_H} = \frac{c\rho A\kappa\Delta T}{kH}\overline{\cos kxT_z}|_1 \sim 10^{22}W,$$

and thus for a large ocean, such as the Pacific or Atlantic, the heat flux due to horizontal convection is bounded by $10^{22}\gamma W$ where γ is the proportion of the Earth's surface covered by the ocean.

2.4 How does this Differ from the Rossby Scaling?

Recall that Rossby [5] proposed a scaling for the boundary layer, in which $\partial/\partial z \sim \delta^{-1}$, $\partial/\partial x \sim 1$ and $\mathbf{u} \sim (\delta^{-2}, 0, \delta^{-1})$. With this scaling $Nu_H \sim \langle|\boldsymbol{\nabla}T|^2\rangle \sim R_H^{1/5}$, whereas our rigorous bound only gives $Nu_H \lesssim C_0 R_H^{1/3}$ for a constant C_0.

It turns out that the difference in the scalings comes in the bound for $\langle -b\theta\mathbf{u}\cdot\boldsymbol{\nabla}\tau\rangle$, specifically when we come to estimate $\int_{1-\delta_1}^1 |w\theta|dz$. Our estimate (28) bounds this quantity by

$$\frac{2\delta_1^2}{\pi^2}\left(c\int_{1-\delta_1}^1 w_z^2dz + \frac{1}{c}\int_{1-\delta_1}^1 \theta_z^2dz\right).$$

The problem comes in the next step when we estimate

$$\int_{1-\delta_1}^1 w_z^2dz \leq \frac{1}{4}\int_{1-\delta_1}^1 |\boldsymbol{\nabla}\mathbf{u}|^2dz.$$

In fact Rossby's scalings would have

$$\int_{1-\delta_1}^1 w_z^2dz \sim \delta_1^2\int_{1-\delta_1}^1 |\boldsymbol{\nabla}\mathbf{u}|^2dz,$$

since the term on the right hand side is dominated by $\int_{1-\delta_1}^1 u_z^2dz$. If we could show that $\int_{1-\delta_1}^1 w_z^2 \leq K\delta_1^2\int_{1-\delta_1}^1 |\boldsymbol{\nabla}\mathbf{u}|^2dz$ (for some order 1 constant K), then we too would obtain a $R_H^{1/5}$ scaling of the horizontal Nusselt number. However, there is no obvious way to improve the estimate, and so the bound of order $R_H^{1/3}$ stands.

3 Fixed Temperature on the Bottom Boundary

We now consider the problem as shown in figure 1 with a fixed temperature $T = T_0$ at the bottom boundary. We try to bound the horizontal Nusselt number (4). The "conduction" solution T_c is

$$T_c = T_0(1-z) + \frac{\sinh kz\cos kx}{\sinh k},$$

meaning that

$$\overline{\cos kxT_{cz}}|_1 = \frac{k}{2}\coth k. \tag{15}$$

We proceed in the same way as for the fixed flux case, letting $T = \tau(x,z) + \theta(\mathbf{x},t)$ and constructing the functional

$$\mathcal{L} = \overline{\cos kxT_z}|_1 - \langle a\mathbf{u}\cdot(\mathcal{NS})\rangle - \langle b\theta\cdot(\mathcal{H})\rangle.$$

We have $\langle wT\rangle = -T_0 - \overline{T}_z|_0$, but in this case, unlike the fixed flux, we cannot use a bounding principle on T to bound this term, as in section 2.1, because we need to know $\overline{T}_z|_0$. So we must proceed in a similar way to section 2.2 and choose the background field to minimize the worst case estimate of

$$\langle(a\sigma R_H - T_0)w\theta - b\theta\mathbf{u}\cdot\boldsymbol{\nabla}\tau\rangle,$$

which we bound by $\alpha\langle|\boldsymbol{\nabla}\mathbf{u}|^2\rangle + \beta\langle|\boldsymbol{\nabla}\theta|^2\rangle$. Again, we let $T = \tau + \theta$ and choose $\tau = \tau_0(z) + \tau_1(z)\cos kx$ that make the integrand zero over the bulk of the layer, and again τ_1 is given by (7). However, in this case it is not clear whether or not it is best to have just a single boundary layer at the bottom for τ_0 or to have boundary layers top and bottom, since with both options we can force the integrand to be zero over the bulk of the layer whilst satisfying the boundary conditions. However, we obtain the same *scaling* in each case, it is just the *prefactor* that may be improved. For simplicity and comparison with the fixed flux case, we just have a boundary layer at the bottom and let

$$\tau_0 = \begin{cases} \frac{1}{\delta_0}\left(T_0(\delta_0 - z) - \frac{1}{b}(a\sigma R_H - T_0)(1-\delta_0)z\right), & \text{for } 0 < z < \delta_0, \\ -\frac{1}{b}(a\sigma R_H - T_0)(1-z), & \text{for } \delta_0 < z < 1. \end{cases} \tag{16}$$

Proceeding as for the fixed flux case, solving the Euler–Lagrange equations we obtain the extremal bound

$$\mathcal{L} \leq \langle|\boldsymbol{\nabla}\tau|^2\rangle + \frac{(b-2)^2}{4(b-1-\beta)}\langle\boldsymbol{\nabla}\tau\cdot\boldsymbol{\nabla}(\tau - T_c)\rangle - T_0^2 + \frac{(a\sigma R_H - T_0)^2}{4(a\sigma - \alpha)}\frac{k^2\delta_1^5}{504}(1 + O(\delta_1)), \tag{17}$$

where

$$\alpha = \frac{1}{2\pi^2}\max\left(|a\sigma R_H + (b-1)T_0|\,\delta_0 c_0, b\delta_1 c_1(1+2k\delta_1)\right), \tag{18}$$

$$\beta = \frac{2}{\pi^2}\max\left(|a\sigma R_H + (b-1)T_0|\,\frac{\delta_0}{c_0}, \frac{b\delta_1}{c_1}(1+2k\delta_1)\right). \tag{19}$$

Making the simplifying assumption $b = 2$ (though this is not optimal) yields

$$\mathcal{L} \leq \frac{1}{4}\left(\frac{1}{\delta_0} - 1\right)(a\sigma R_H + T_0)^2 + \frac{1}{2\delta_1} + \frac{k^2\delta_1}{6} + \frac{(a\sigma R_H - T_0)^2}{4(a\sigma - \alpha)}\frac{k^2\delta_1^5}{504}(1 + O(\delta_1)). \tag{20}$$

For moderate T_0, where we expect $\delta_0 \ll 1$ and $\delta_1 \ll 1$, it may be shown that the dominant contribution to the bound is given by G where

$$G = \frac{1}{4\delta_0}(a\sigma R_H + T_0)^2 + \frac{1}{2\delta_1}.$$

For the bound to be as tight as possible, we need to choose δ_0 and δ_1 as large as possible. Subject to the spectral constraints, the best choice is $a\sigma = 4\delta_1^2/\pi^4$ and $\delta_0 = 2\delta_1/|4\delta_1^2 R_H/\pi^4 + T_0|$, meaning that

$$G = \frac{1}{8\delta_1}\left|\frac{4\delta_1^2 R_H}{\pi^4} + T_0\right|^3 + \frac{1}{2\delta_1}.$$

Assuming that $x = 4\delta_1^2 R_H/\pi^4 + T_0 > 0$, (which can be checked) we have

$$\frac{dG}{d\delta_1} = \frac{1}{8\delta_1^2}\left(5x^3 - 6T_0x^2 - 4\right).$$

It may be shown that there is only one positive root $x = x^*$ of $dG/d\delta_1 = 0$, which provides the minimum of G, giving the bound

$$\boxed{Nu_H \lesssim R_H^{1/2} f(T_0),} \tag{21}$$

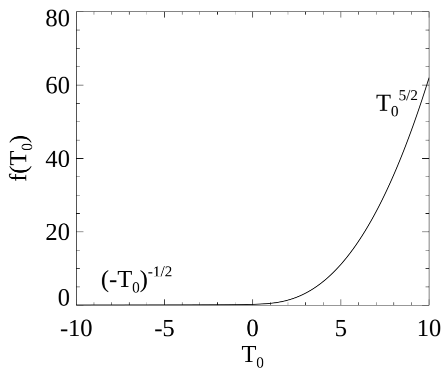

(a)

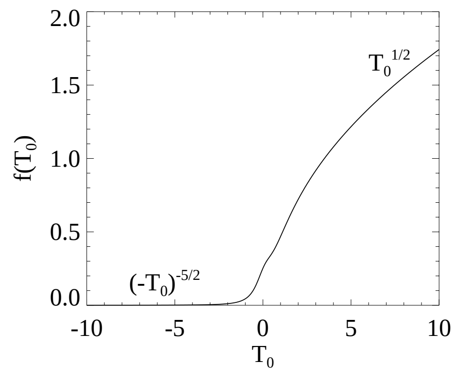

(b)

Figure 5: Prefactor for the bound on the Nusselt number with fixed temperature T_0 at the bottom of the layer and $k = 1.25 \times 10^{-3}$. The bound is proportional to $R_H^{1/2}$ in each case. (a) shows the prefactor with the horizontal Nusselt number $Nu_H = \overline{\cos kxT_z}|_1/\overline{\cos kxT_{cz}}|_1$, whilst (b) shows the prefactor with Nusselt number $Nu = \langle|\boldsymbol{\nabla}T|^2\rangle/\langle|\boldsymbol{\nabla}T_c|^2\rangle$.

where

$$f(T_0) = \frac{x^{*3} + 4}{2\pi^2\sqrt{(x^* - T_0)}k \coth k},$$

as long as $|T_0| \ll R_H$. A graph of f is shown in figure 5(a).

For $T_0 \gg 0$, the leading order contribution comes from the first term in (20) and we pick $a\sigma = T_0/5R_H$ and $\delta_0 = \sqrt{5}\pi^2/6\sqrt{R_H T_0}$, giving

$$Nu_H \lesssim \frac{108 T_0^{5/2} R_H^{1/2}}{25\sqrt{5}\pi^2 k \coth k}.$$

For $T_0 \ll 0$, we may set $\delta_0 = \delta_1 = 1$ and the dominant contribution is from the term $(1 + O(\delta_1))(a\sigma R_H - T_0)^2 k^2 \delta_1^5/2016(a\sigma - \alpha)$. This is of order $-T_0 R_H k^2$ multiplied by some prefactor, but to work out this prefactor we would have to solve (31) in appendix B to all orders. So the most we can say without doing the full calculation is that the bound on the horizontal Nusselt number is of order $-T_0 R_H$.

3.1 Connection to Rayleigh–Bénard Scaling

For very large T_0 we would expect the motion to be dominated by the large vertical temperature gradient and look like Rayleigh–Bénard convection, and thus would expect the vertical Nusselt number to be bounded by $R_V^{1/2}$ multiplied by some prefactor, (where $R_V = T_0 R_H$ is the vertical Rayleigh number). Similarly in the limit of small T_0, we would expect the Nusselt number to be bounded by something that tends to unity.

In order to check that the bounds match in the two limits, we define the Nusselt number to be

$$Nu = \frac{\langle|\boldsymbol{\nabla}T|^2\rangle}{\langle|\boldsymbol{\nabla}T_c|^2\rangle},$$

and proceed to try to bound it. In this case

$$\langle |\boldsymbol{\nabla} T_c|^2 \rangle = T_0^2 + \frac{1}{2} k \coth k.$$

This time instead of (20), we obtain the expression

$$\mathcal{L} \leq \frac{1}{\delta_0} \left(a\sigma R_H + T_0 \right)^2 - \frac{1}{4} a\sigma R_H (a\sigma R_H + 4T_0) + \frac{1}{2\delta_1} + \frac{k^2 \delta_1}{6} + \frac{(a\sigma R_H - T_0)^2}{4(a\sigma - \alpha)} \frac{k^2 \delta_1^5}{504} (1 + O(\delta_1)). \quad (22)$$

For moderate T_0, we obtain (21) again, but this time $f(T_0)$ is given by the graph in figure 5(b). If $T_0 \gg 1$ then

$$Nu \lesssim \frac{216}{25\pi^2} \sqrt{\frac{2}{5}} \sqrt{T_0 R_H} = \frac{216}{25\pi^2} \sqrt{\frac{2}{5}} \sqrt{R_V} \approx 0.55 R_V^{1/2}.$$

to leading order and thus we recover the scaling of the Doering–Constantin result for Rayleigh–Bénard convection [12], although the prefactor is not optimal since we only used a *bottom* boundary layer and not a top one. If we use top and bottom boundary layers of equal depth, and optimize over the choices of constants a, b, δ_0, δ_1, then we get $Nu_H \lesssim 3\sqrt{3} R_V^{1/2} / 4\pi^2 \approx 0.13 R_V^{1/2}$ at leading order, and the prefactor agrees with the Rayleigh–Bénard result.

If $T_0 \ll -R_H$ then we can choose $\delta_0 = 1$, and the leading order contribution is from the first two terms in the bound (22), which gives $\mathcal{L} \lesssim T_0^2$ and hence

$$Nu \lesssim 1,$$

to leading order, and so we also recover the result for Rayleigh–Bénard convection in the limit of small T_0.

4 Intermediate Bottom Boundary Condition

We now wish to see more clearly why the $R_H^{1/3}$ and $R_H^{1/2}$ scalings arise – what is the connection between them and what happens if we have a boundary condition that is not perfectly conducting or perfectly insulating?

We choose the bottom boundary condition $T - \lambda T_z = T_0$ at $z = 0$, where $\lambda \geq 0$, smoothly moving from a perfectly insulating condition at $\lambda = \infty$ to a perfectly conducting condition for $\lambda = 0$. This physically corresponds to the bottom of the layer being in contact with a thin imperfectly conducting sheet that is in contact with an infinite heat bath. For this boundary condition, it is not immediately obvious that the velocity and temperature fields stay bounded and thus we first prove their boundedness, which enables us to drop the averages of their time derivatives.

4.1 Bounds on the Temperature and Velocity Fields

In this section, we prove that the fields are bounded in time, which is not completely obvious for the given boundary conditions. Thus for this section only (section 4.1), $\langle\cdot\rangle$ and $\overline{\cdot}$ denote only spatial averages (and not long time average).

First of all we prove a boundedness principle for the temperature field, using ideas from [13]. We consider the solution of $(\mathcal{H})$ starting from some bounded initial temperature distribution at $t = 0$, and solved on the time interval $t \in [0, t_0]$. We want to look for the point where T attains its maximum value. Suppose the maximum occurs at a point where $z \neq 0, 1$. At this point we must have $\boldsymbol{\nabla} T = 0$, $\nabla^2 T \leq 0$ and so from $(\mathcal{H})$, $\partial T/\partial t \leq 0$, meaning that the maximum of T is attained at $t = 0$. If the maximum occurs at $z = 0$, then we have $T_z \leq 0$ there, which implies, using the boundary condition, that $T \leq T_0$. Alternatively it can occur at $z = 1$, in which case $T \leq 1$. A similar principle can be used to bound T from below and thus T is everywhere in the range

$$[\min(-1, T_0, \inf(T|_{t=0})), \max(1, T_0, \sup(T|_{t=0}))].$$

If the system is allowed to relax for sufficiently long then T will eventually be in the range

$$[\min(-1, T_0), \max(1, T_0)],$$

a result that we shall use when applying the background method.

To bound the velocity field, we first use Poincaré's inequality and obtain $\langle|\mathbf{u}|^2\rangle \leq 2\langle|\boldsymbol{\nabla}\mathbf{u}|^2\rangle/\pi^2$. Rearranging $\langle\mathbf{u}\cdot(\mathcal{NS})\rangle$ yields averaging yields

$$\begin{aligned}
\frac{1}{2}\frac{d}{dt}\langle|\mathbf{u}|^2\rangle &= R_H\langle wT\rangle - \langle|\boldsymbol{\nabla}\mathbf{u}|^2\rangle, \\
&\leq R_H\sqrt{\langle w^2\rangle\langle T^2\rangle} - \langle|\boldsymbol{\nabla}\mathbf{u}|^2\rangle, \\
&\leq R_H\sqrt{\langle|\mathbf{u}|^2\rangle\langle T^2\rangle} - \langle|\boldsymbol{\nabla}\mathbf{u}|^2\rangle, \\
\Rightarrow \quad \frac{d}{dt}\sqrt{\langle|\mathbf{u}|^2\rangle} &\leq R_H\sqrt{\langle T^2\rangle} - \frac{\langle|\boldsymbol{\nabla}\mathbf{u}|^2\rangle}{\sqrt{\langle|\mathbf{u}|^2\rangle}}, \\
&\leq R_H\sqrt{\langle T^2\rangle} - \frac{2}{\pi^2}\sqrt{\langle|\mathbf{u}|^2\rangle},
\end{aligned}$$

meaning that $\langle|\mathbf{u}|^2\rangle$ is bounded above by its initial value and $\pi^2 R_H\sqrt{\langle T^2\rangle}/2$.

4.2 The Set Up

Having proved the boundedness of the fields, we can now begin to apply the Doering–Constantin method to bound the horizontal Nusselt number given by (4). With these boundary conditions, T_c is given by

$$T_c = T_0\left(\frac{1-z}{1+\lambda}\right) + \frac{\sinh kz + \lambda k\cosh kz}{\sinh k + \lambda k\cosh k}\cos kx,$$

giving

$$\overline{\cos kx T_{cz}}|_1 = \frac{k}{2}\left(\frac{\cosh k + \lambda k\sinh k}{\sinh k + \lambda k\cosh k}\right),$$

and so we try to find an upper bound on the numerator of Nu_H

$$\overline{\cos kxT_z}|_1 = \langle |\boldsymbol{\nabla} T|^2\rangle + \overline{T(T-T_0)}|_0/\lambda.$$

Letting $T = \tau + \theta$, where τ satisfies the boundary conditions on T and θ satisfies the homogeneous boundary conditions, we have

$$\begin{aligned}
\mathcal{L} =& \overline{\cos kxT_z}|_1 - \langle a\mathbf{u}\cdot(\mathcal{NS})\rangle - \langle b\theta\cdot(\mathcal{H})\rangle, \\
=& \langle |\boldsymbol{\nabla}\tau|^2 - a\sigma|\boldsymbol{\nabla}\mathbf{u}|^2 + (b-1)\theta\nabla^2\theta + (b-2)\theta\nabla^2\tau + a\sigma R_H w(\tau+\theta) \\
& - b\theta\mathbf{u}\cdot\boldsymbol{\nabla}\tau\rangle - \overline{\theta\theta_z}|_0 - 2\overline{\theta\tau_z}|_0 + \frac{1}{\lambda}\overline{T(T-T_0)}|_0, \\
=& \langle |\boldsymbol{\nabla}\tau|^2 - a\sigma|\boldsymbol{\nabla}\mathbf{u}|^2 + (b-1)\theta\nabla^2\theta + (b-2)\theta\nabla^2\tau + a\sigma R_H w(\tau+\theta) \\
& - b\theta\mathbf{u}\cdot\boldsymbol{\nabla}\tau\rangle + \frac{1}{\lambda}\overline{(\tau-T_0)^2}|_0 + \frac{T_0}{\lambda}(\overline{T}|_0 - T_0), \qquad (23) \\
=& \langle |\boldsymbol{\nabla}\tau|^2 - a\sigma|\boldsymbol{\nabla}\mathbf{u}|^2 + (b-1)\theta\nabla^2\theta + (b-2)\theta\nabla^2\tau + \mu w(\tau+\theta) \\
& - b\theta\mathbf{u}\cdot\boldsymbol{\nabla}\tau\rangle + \frac{1}{\lambda}\overline{(\tau-T_0)^2}|_0 - \frac{T_0^2}{1+\lambda}. \qquad (24)
\end{aligned}$$

where

$$\mu = a\sigma R_H - \frac{T_0}{1+\lambda},$$

and we have used the lower boundary conditions to obtain (23). Then to obtain (24), the final term in (23) can be absorbed into the global average, using $(\mathcal{H})$ to derive an expression for $\overline{T}|_0$:

$$\langle wT\rangle = -\overline{T}|_0 - \overline{T_z}|_0 = \frac{T_0}{\lambda} - \frac{1+\lambda}{\lambda}\overline{T}|_0 \quad\Rightarrow\quad \overline{T}|_0 = \frac{T_0 - \lambda\langle wT\rangle}{1+\lambda}. \qquad (25)$$

Note also that in (24) we have chosen to rewrite any terms proportional to $|\boldsymbol{\nabla}\theta|^2$ in terms of $\theta\nabla^2\theta$. This is because when the Euler–Lagrange equations are computed to minimize such terms, the former term would give some contributions from the boundary, which make the equation more difficult to solve, whereas the latter will not.

4.3 Bound on the Horizontal Nusselt Number

Starting from expression (24), we proceed to try to minimize $\mathcal{L}$ using the boundedness of the temperature. From (25) we can bound $\langle \mu w(\tau+\theta)\rangle = \mu\langle wT\rangle \le M\mu$, where

$$M = \begin{cases} \max\left(\frac{T_0+1+\lambda}{\lambda}, -T_0\right), & \text{if } \mu \ge 0, \\ \max\left(\frac{T_0-1-\lambda}{\lambda}, -T_0\right), & \text{if } \mu \le 0. \end{cases}$$

We choose the background field τ to minimize the worst case estimate of $\langle -b\theta\mathbf{u}\cdot\boldsymbol{\nabla}\tau\rangle$, choosing $\boldsymbol{\nabla}\tau = 0$ over as much as possible of the layer. In order to satisfy the boundary conditions we must again have top and bottom boundary layers. We choose τ_1 to be given by (7) and

$$\tau_0 = \begin{cases} \frac{\delta_0 - z}{\delta_0+\lambda}T_0, & \text{for } 0 < z < \delta_0, \\ 0, & \text{for } \delta_0 < z < 1, \end{cases}$$

With this choice,

$$\langle -b\theta\mathbf{u}\cdot\boldsymbol{\nabla}\tau\rangle \le \alpha\langle|\boldsymbol{\nabla}\mathbf{u}|^2\rangle + \beta\langle|\boldsymbol{\nabla}\theta|^2\rangle,$$

for all fields $\mathbf{u}$ and θ where, using the estimates in appendix A,

$$\begin{aligned}
\alpha &= b\max\left(\frac{|T_0|}{\delta_0+\lambda}\frac{\delta_0^2 c_0}{2\pi^2}, \frac{\delta_1 c_1}{2\pi^2}(1+2k\delta_1)\right),\\
\beta &= b\left(\frac{|T_0|}{\delta_0+\lambda}\frac{\delta_0}{2c_0} + \frac{2\delta_1}{\pi^2 c_1}(1+2k\delta_1)\right).
\end{aligned}$$

Then

$$\begin{aligned}
\mathcal{L} \le \Big\langle |\boldsymbol{\nabla}\tau|^2 - (a\sigma-\alpha)|\boldsymbol{\nabla}\mathbf{u}|^2 + (b-1-\beta)\theta\nabla^2\theta + (b-2)\theta\nabla^2\tau\Big\rangle&\\
+ M\mu + \frac{1}{\lambda}\overline{(\tau-T_0)^2}|_0 - \frac{T_0^2}{1+\lambda}&,
\end{aligned}$$

where the boundary term $-\beta\overline{\theta\theta_z}|_0$ arising from the integration by parts has been neglected since it is negative semi-definite as long as $\beta,\lambda \ge 0$.

The Euler–Lagrange equations for minimization of the functional bound for $\mathcal{L}$ are

$$\begin{aligned}
\boldsymbol{\nabla}p - 2(a\sigma-\alpha)\nabla^2\mathbf{u} &= 0,\\
-2(b-1-\beta)\nabla^2\theta &= (b-2)\nabla^2\tau,
\end{aligned}$$

yielding the solution

$$\mathbf{u}^* = 0, \quad \theta^* = \frac{-(b-2)}{2(b-1-\beta)}(\tau - T_c),$$

which minimizes the functional as long as the spectral constraints $a\sigma \ge \alpha$ and $b-1 \ge \beta$ are satisfied. The extremal bound is

$$\begin{aligned}
\mathcal{L} \le \langle|\boldsymbol{\nabla}\tau|^2\rangle + \frac{(b-2)^2}{4(b-1-\beta)}\left(\langle\boldsymbol{\nabla}\tau\cdot\boldsymbol{\nabla}(\tau-T_c)\rangle + \frac{1}{\lambda}\overline{(\tau-T_c)(\tau-T_0)}|_0\right)&\\
+ M\mu + \frac{1}{\lambda}\overline{(\tau-T_0)^2}|_0 - \frac{T_0^2}{1+\lambda}&,
\end{aligned}$$

and similarly to section 2.1 we can show that $b = 2$ is the value giving the tightest bound. We also have

$$\begin{aligned}
\langle|\boldsymbol{\nabla}\tau|^2\rangle &= \frac{\delta_0 T_0^2}{(\delta_0+\lambda)^2} + \frac{1}{2\delta_1} + \frac{k^2\delta_1}{6},\\
\overline{(\tau-T_0)^2}|_0 &= \frac{\lambda^2 T_0^2}{(\delta_0+\lambda)^2}.
\end{aligned}$$

In the following, we only consider the bounds as $R_H \to \infty$ with T_0 and λ fixed; if R_H is finite, it may be that a better bound can be obtained with a different scaling. As in section 2.1, the choice $\delta_0 = 0$ does not affect the bound at leading order and subject to the spectral constraint, the optimal value of $a\sigma$ is $4\delta_1^2/\pi^4$ to leading order, giving $\mathcal{L} \lesssim$

$1/2\delta_1 + 4M\delta_1^2 R_H/\pi^4$. The tightest bound is obtained with $\delta_1 = (\pi/2)^{4/3}(MR_H)^{-1/3}$, giving $\mathcal{L} \leq 3(MR_H)^{1/3}/2^{2/3}\pi^{4/3}$ and so the horizontal Nusselt number is bounded by

$$\boxed{Nu_H \lesssim \begin{cases} 3 \cdot 2^{1/3}(-T_0 R_H)^{1/3} \Big/ \pi^{4/3} k \left(\frac{\cosh k + \lambda k \sinh k}{\sinh k + \lambda k \cosh k}\right), & \text{if } T_0 \leq -1, \\ 3 \cdot 2^{1/3} \left(\frac{T_0+1+\lambda}{\lambda} R_H\right)^{1/3} \Big/ \pi^{4/3} k \left(\frac{\cosh k + \lambda k \sinh k}{\sinh k + \lambda k \cosh k}\right), & \text{if } T_0 \geq -1. \end{cases}} \tag{26}$$

If we proceed without utilising the boundedness of the temperature field, then as with the fixed flux case, the bound on Nu_H is proportional to $R_H^{2/5}$, and so the $R_H^{1/3}$ bound is always better as $R_H \to \infty$ with T_0 and λ fixed.

As $\lambda \to \infty$ with $T_0/\lambda = F$ fixed, we immediately recover the bound for the fixed flux bottom boundary condition (11) in section 2.1. As $\lambda \to 0$, we might similarly hope to recover the bounds found in section 3. However, things are not so simple as we might expect!

4.4 Bound for Small λ and Connection to Fixed Temperature Boundary Condition?

As long as $\lambda > 0$, then (26) shows that we have a bound of size $R_H^{1/3}$. However, if $\lambda = 0$, then as shown in section 3 we can only get a bound of order $R_H^{1/2}$. Why do we have this difference?

In fact, as $\lambda \to 0$, both the bounds in (26) grow arbitrarily large (if $T_0 \leq -1$ then this growth is in one of the omitted terms) and so, although the asymptotic behavior is $R_H^{1/3}$, for any finite value of R_H, the prefactor is so huge that the bound will be larger than might be expected. Thus we may ask ourselves, whether there is some way to make the bounds connect in the limit of small λ by using a different background field.

The bounds on T at $z = 0$ provide poor estimates for small λ (unless $T_0 = 0$), and so we shall do better if we proceed without using this. Starting from the expression (24), we choose the background field τ to make the integrand of the unwanted terms $\langle \mu w\theta - b\theta \mathbf{u}\cdot\boldsymbol{\nabla}\tau\rangle$ zero over as much of the layer as possible. Again we set $\tau = \tau_0(z) + \tau_1(z)\cos kx$ where τ_1 is given by (7) and

$$\tau_0 = \begin{cases} \frac{1}{\delta_0+\lambda}\left(T_0(\delta_0 - z) - \frac{\mu}{b}(1-\delta_0)(z+\lambda)\right), & \text{for } 0 < z < \delta_0, \\ -\frac{\mu}{b}(1-z), & \text{for } \delta_0 < z < 1, \end{cases}$$

which tends to the expression for fixed temperature (16) in the limit $\lambda \to 0$. Solving the Euler–Lagrange equations yields the bound

$$\mathcal{L} \leq \langle|\boldsymbol{\nabla}\tau|^2\rangle + \frac{(b-2)^2}{4(b-1-\beta)}\left(\langle\boldsymbol{\nabla}\tau\cdot\boldsymbol{\nabla}(\tau - T_c)\rangle + \frac{1}{\lambda}\overline{(\tau - T_c)(\tau - T_0)}|_0\right) + \frac{1}{\lambda}\overline{(\tau - T_0)^2}|_0$$
$$- \frac{T_0^2}{1+\lambda} + \frac{\mu^2}{4(a\sigma - \alpha)}\frac{k^2\delta_1^5}{504}(1 + O(\delta_1)),$$

which tends to expression (17) as $\lambda \to 0$. Using appendix A, the estimates for α and β are

$$\alpha = \max\left(\frac{|\mu(\lambda+1)+bT_0|}{\delta_0+\lambda}\frac{\delta_0^2 c_0}{2\pi^2}, \frac{b\delta_1 c_1}{2\pi^2}(1+2k\delta_1)\right),$$
$$\beta = \frac{|\mu(\lambda+1)+bT_0|}{\delta_0+\lambda}\frac{\delta_0}{2c_0} + \frac{2b\delta_1}{\pi^2 c_1}(1+2k\delta_1).$$

Comparing these with (18) and (19) respectively, we see that as $\lambda \to 0$ we obtain the same limit for the second term in each expression, but not the first term. This is due to the fact that with the methods we have used, we cannot estimate the temperature on the lower boundary very well, and so we are forced to use the bound (30) rather than (29). This difference turns out to be crucial in the bounding procedure and thus we cannot obtain a continuous bound on the horizontal Nusselt number as $\lambda \to 0$.

5 Conclusions and Discussion

In summary, we have obtained upper bounds on the horizontal Nusselt number for horizontal convection using a variety of different boundary conditions on the bottom of the box. As long as the lower boundary is not perfectly conducting we found that the horizontal Nusselt number is always bounded by a constant prefactor times $R_H^{1/3}$, and if it is perfectly conducting then the bound increases to a prefactor times $R_H^{1/2}$.

In a similar way, we might ask if it is possible to use the analogous method to bound the dissipation ϵ. However, it turns out that we cannot improve on the bound obtained using the method outlined in the introduction. For a fixed heat flux F through the bottom, we get

$$\epsilon \leq \frac{\kappa g \alpha \Delta T}{H}(1+F),$$

and for the intermediate boundary conditions, we get

$$\epsilon \leq \frac{\kappa g \alpha \Delta T}{H} \max\left(\frac{T_0+1+\lambda}{\lambda}, -T_0\right).$$

These bounds imply the anti-turbulence theorem in both cases. With the fixed temperature boundary condition, however, we can't easily relate the flux through the bottom to the temperature there, and in this case, using the Doering–Constantin method, the bound turns out to be $\langle|\nabla \mathbf{u}|^2\rangle \leq g(T_0)R^{3/2}$ for some function g, meaning that ϵ is bounded by a non-zero constant as $\kappa \to 0$ with σ fixed, which does not prove anti-turbulence.

It would be interesting to have some idea of what the actual velocity and temperature fields look like in the asymptotic limit as $R_H \to \infty$, and see if figure 4 does indeed give the correct flow pattern in the limit. However, since we set the velocity to zero, the method we have used tells us nothing about the velocity field except perhaps that the velocities in the asymptotic solution are not very large in magnitude. It doesn't prove anything about the temperature field either, although the fact that we did consistently use the background field $\tau = \tau_0(z) + \tau_1(z)\cos kx$ where τ_1 was given by (7), suggests that the real solution may have a top boundary layer and that the temperature field has little horizontal dependence deeper into the layer. Our choice of τ_0 varied but we found that the depth of the bottom boundary layer did not matter at leading order, (except with the fixed bottom temperature condition), suggesting that the horizontally averaged temperature has no large gradients throughout the layer.

Possibly a more physically realistic set up in the oceanographic context would be to use a stress free velocity boundary condition at the top of the layer rather than the non-slip one, shown in 1, which was used throughout the report. Proceeding to bound the horizontal Nusselt number in a similar fashion, we encounter a problem. We cannot estimate $\int_{1-\delta}^{1} \overline{|u\theta|}dz$ in terms of $\langle|\boldsymbol{\nabla}\mathbf{u}|^2\rangle$ and $\langle|\boldsymbol{\nabla}\theta|^2\rangle$ as we have no control on the size of u at the top boundary, and so we cannot easily find a bound on Nu_H. Note that this problem does not occur for Rayleigh–Bénard convection, since the offending term only arises due to the horizontal dependence of τ.

In summary the bound of $R_H^{1/3}$, (which holds asymptotically for all the boundary conditions investigated except for the fixed temperature condition), suggests that horizontal convection with an insulating or nearly insulating bottom boundary is much less efficient at transporting heat through a layer than Rayleigh–Bénard convection. In particular, since the bound less than order $R_H^{1/2}$, the scalings of the temperature and velocity fields in the boundary layers in horizontal convection cannot be independent of the molecular parameters ν and κ [14, 15].

So how relevant are these results to the ocean? We don't know the oceanographic bottom boundary conditions, and the bottom is certainly far from being flat! However, we have shown that there is only a weak dependence on these conditions, and so the results are probably still valid. However, possibly more significantly, there are many other processes going on in the ocean such as wind forcing, that can cause large amounts of mixing and these are probably much more significant factors in the circulation than horizontal convection.

I should like to thank Richard Kerswell for suggesting this project and for giving up a lot of time to discuss the problem, Neil Balmforth who provided many useful insights and Charles Doering for making some helpful suggestions. I am grateful to Woods Hole Oceanographic Institution for its funding and hospitality and to everyone on the GFD program for making my stay so enjoyable!

A Estimates of Boundary Layer Integrals

In this section we estimate the maximum possible size of some integrals that are needed to estimate the sign-indeterminate quadratic terms. The integrals that are needed are

$$\int_{1-\delta}^{1} \overline{|w\theta|}dz, \quad \int_{1-\delta}^{1} \overline{|u\theta|}dz \quad \text{and} \int_{0}^{\delta} \overline{|w\theta|}dz,$$

where u and w are zero on both the top and bottom boundaries and θ is zero at the top. At the bottom we have three possibilities: $\theta = 0$, $\theta_z = 0$ or $\theta - \lambda\theta_z = 0$.

First we prove the result

If the functions f and g are both zero on the plane $z = z_0$ then

$$\int_{z_0}^{z_0+\delta} \overline{|fg|}dz \leq \frac{2\delta^2}{\pi^2}\left(c\int_{z_0}^{z_0+\delta} \overline{f_z^2}dz + \frac{1}{c}\int_{z_0}^{z_0+\delta} \overline{g_z^2}dz\right).$$

The proof (thanks to Michael Proctor) is as follows:

$$\begin{aligned}
\int_{z_0}^{z_0+\delta} \overline{|fg|}dz \leq & \overline{\left(\int_{z_0}^{z_0+\delta} f^2dz \int_{z_0}^{z_0+\delta} g^2dz\right)^{1/2}}, \\
& \text{(using the Cauchy–Schwarz inequality)}, \\
\leq & \frac{1}{2}\left(c\int_{z_0}^{z_0+\delta} \overline{f^2}dz + \frac{1}{c}\int_{z_0}^{z_0+\delta} \overline{g^2}dz\right), \\
& \text{(using Young's inequality, } \sqrt{ab} \leq (ca + b/c)/2 \text{ for any } c > 0).
\end{aligned}$$

We can use the calculus of variations to minimize the ratio

$$\int_{z_0}^{z_0+\delta} h_z^2 dz \Big/ \int_{z_0}^{z_0+\delta} h^2 dz,$$

subject to $h(z_0) = 0$. The minimum value is $\pi^2/4\delta^2$, and hence the result follows.

Using this we have

$$\int_{1-\delta}^{1} \overline{|u\theta|}dz \leq \frac{2\delta^2}{\pi^2}\int_{1-\delta}^{1}\left(c\overline{u_z^2} + \frac{\overline{\theta_z^2}}{c}\right)dz \leq \frac{2\delta^2}{\pi^2}\int_{1-\delta}^{1}\left(c\overline{|\boldsymbol{\nabla}\mathbf{u}|^2} + \frac{1}{c}\overline{|\boldsymbol{\nabla}\theta|^2}\right)dz, \tag{27}$$

$$\int_{1-\delta}^{1} \overline{|w\theta|}dz \leq \frac{2\delta^2}{\pi^2}\int_{1-\delta}^{1}\left(c\overline{w_z^2} + \frac{\overline{\theta_z^2}}{c}\right)dz \leq \frac{2\delta^2}{\pi^2}\int_{1-\delta}^{1}\left(c\overline{w_z^2} + \frac{1}{c}\overline{|\boldsymbol{\nabla}\theta|^2}\right)dz, \tag{28}$$

and similarly if $\theta = 0$ at $z = 0$ then

$$\int_{0}^{\delta} \overline{|w\theta|}dz \leq \frac{2\delta^2}{\pi^2}\int_{0}^{\delta}\left(c\overline{w_z^2} + \frac{1}{c}\overline{|\boldsymbol{\nabla}\theta|^2}\right)dz, \tag{29}$$

otherwise

$$\begin{aligned}
\int_{0}^{\delta} \overline{|w\theta|}dz \leq & \overline{\left(\int_0^\delta w^2dz \int_0^\delta \theta^2 dz\right)^{1/2}}, \text{ (Cauchy–Schwartz)}, \\
\leq & \frac{1}{2}\left(c\int_0^\delta \overline{w^2}dz + \frac{1}{c}\int_0^\delta \overline{\theta^2}dz\right), \text{ (Young's inequality)}, \\
\leq & \frac{1}{2}\left(\frac{4\delta^2 c}{\pi^2}\int_0^\delta \overline{w_z^2}dz + \frac{1}{c}\int_0^\delta \overline{\left(\int_z^1 \theta_{z'}dz'\right)^2}dz\right), \\
\leq & \frac{2\delta^2 c}{\pi^2}\int_0^\delta \overline{w_z^2}dz + \frac{1}{2c}\int_0^\delta \overline{\left((1-z)\int_z^1 \theta_{z'}^2 dz'\right)}dz, \text{ (Cauchy–Schwartz)}, \\
\leq & \frac{2\delta^2 c}{\pi^2}\int_0^\delta \overline{w_z^2}dz + \frac{\delta}{2c}\langle|\boldsymbol{\nabla}\theta|^2\rangle,
\end{aligned} \tag{30}$$

where c can take any positive value.

Rather than simply bounding w_z^2 by $|\boldsymbol{\nabla}\mathbf{u}|^2$, we improve the bounds by using the following inequality, which is taken from [12]. Since $u_x + v_y + w_z = 0$ then

$$\langle u_x w_z + v_y w_z + w_z^2\rangle = 0 \Rightarrow \langle u_z w_x + v_z w_y + w_z^2\rangle = 0,$$
$$\langle w_z^2\rangle = \langle(u_x + v_y)^2\rangle \Rightarrow \langle w_z^2 - u_x^2 - v_y^2 - 2u_y v_x\rangle = 0,$$

where the boundary conditions have been used to integrate by parts. Twice the first equation plus the second plus $\langle|\boldsymbol{\nabla}\mathbf{u}|^2\rangle$ gives

$$\langle 4w_z^2 + (u_y - v_x)^2 + (u_z + w_x)^2 + (v_z + w_y)^2\rangle = \langle|\boldsymbol{\nabla}\mathbf{u}|^2\rangle \Rightarrow \boxed{\langle w_z^2\rangle \le \frac{1}{4}\langle|\boldsymbol{\nabla}\mathbf{u}|^2\rangle.}$$

B Estimate of the Size of $\langle w^*\tau\rangle$

In section 2.2, we obtained a term proportional to $\langle w^*\tau\rangle$ in the bounding procedure. This term must be estimated, which is done in this section.

In both cases $\mathbf{u}^*$ satisfies an equation of the form

$$\boldsymbol{\nabla} p - \nabla^2\mathbf{u} = P\tau\hat{\mathbf{z}}, \tag{31}$$

where $\tau = \tau_0(z) + \tau_1(z)\cos kx$ and

$$\tau_1 = \begin{cases} 0, & \text{for } 0 < z < 1-\delta_1, \\ \frac{z-1+\delta_1}{\delta_1}, & \text{for } 1-\delta_1 < z < 1, \end{cases}$$

Taking the curl gives

$$\begin{aligned} \nabla^4\psi &= -P\tau_x, \\ &= \begin{cases} \frac{Pk}{\delta_1} y \sin kx & \text{for } y > 0, \\ 0 & \text{for } y < 0, \end{cases} \end{aligned}$$

where $y = z - 1 + \delta_1$ and $\mathbf{u} = (-\psi_z, 0, \psi_x)$. The solution is of the form

$$\psi = \begin{cases} \frac{P}{k^3\delta_1}\left(y + (A'y+B')\sinh ky + (C'y+D')\cosh ky\right)\sin kx \\ \qquad \text{for } 0 < y < \delta_1, \\ \frac{P}{k^3\delta_1}\left((Ay+B)\sinh ky + (Cy+D)\cosh ky\right)\sin kx \\ \qquad \text{for } -1+\delta_1 < y < 0, \end{cases}$$

for some constants A, B, C, D, A', B', C' and D' to be determined. Note that since ψ is proportional to $\sin kx$, $\langle w^*\tau\rangle = \langle w^*\tau_1\cos kx\rangle$, with no contribution from τ_0 and so the solution is only needed in the top boundary layer.

Matching ψ, ψ_y, ψ_{yy} and ψ_{yyy} at y=0 gives

$$A' = A, \quad B' = B - \frac{3}{2k}, \quad C' = C + \frac{1}{2}, \quad D' = D.$$

The boundary conditions at the top and bottom of the box imply that

$$\begin{pmatrix} \delta_1 s_t & s_t & \delta_1 c_t & c_t \\ s_t + k\delta_1 c_t & kc_t & k\delta_1 s_t + c_t & ks_t \\ (\delta_1 - 1)s_b & s_b & (\delta_1-1)c_b & c_b \\ s_b + k(\delta_1-1)c_b & kc_b & k(\delta_1-1)s_b + c_b & ks_b \end{pmatrix} \begin{pmatrix} A \\ B \\ C \\ D \end{pmatrix}$$
$$= \begin{pmatrix} -\delta_1 + \frac{3}{2k}s_t - \frac{1}{2}\delta_1 c_t \\ -1 - \frac{1}{2}k\delta_1 s_t + c_t \\ 0 \\ 0 \end{pmatrix}, \tag{32}$$

where $c_t = \cosh k\delta_1$, $s_t = \sinh k\delta_1$, $c_b = \cosh k(\delta_1 - 1)$ and $s_b = \sinh k(\delta_1 - 1)$. Note that if $\delta_1 \ll 1$ then the right hand side of this equation is $O(\delta_1^4)$, whilst the determinant of the matrix is $O(1)$, and thus A, B, C and D are $O(\delta_1^4)$ at the largest. In fact the first equation arising from this matrix equation is

$$\delta_1 s_t A + s_t B + \delta_1 c_t C + c_t D = -\delta_1 + \frac{3}{2k} s_t - \frac{1}{2}\delta_1 c_t,$$

The coefficients of the first three terms are at most $O(\delta_1)$, and so the terms must be $O(\delta_1^5)$. The right hand side is also $O(\delta_1^5)$ and c_t is $O(1)$. Thus D is $O(\delta_1^5)$. Therefore since y is $O(\delta_1)$ in the top boundary layer,

$$\begin{aligned}\psi &= \frac{P}{k^3\delta_1}\left(y - \frac{3}{2k}\sinh ky + \frac{1}{2}y\cosh ky + O(\delta_1^5)\right)\sin kx,\\ &= O(P\delta_1^4).\end{aligned}$$

Therefore w is also $O(P\delta_1^4)$ and so

$$\boxed{\langle w^*\tau\rangle = O(P\delta_1^5).} \tag{33}$$

In fact, by inverting the matrix in (32), we have, to leading order

$$\mathbf{u}^* = P\left(\left(\frac{1}{24}(1-\zeta^4)k\delta_1^3 - \frac{(e^{4k} - 4ke^{2k} - 1)(1-\zeta)k^2\delta_1^4}{12((e^{2k}-1)^2 - 4k^2e^{2k})} + O(\delta_1^5)\right)\sin kx,\right.$$
$$\left. 0, \left(\frac{k^2}{120}(4 - 5\zeta + \zeta^5)\delta_1^4 + O(\delta_1^5)\right)\cos kx\right),$$

in the top boundary layer, where $\zeta = y/\delta_1 > 0$, giving

$$\langle w^*\tau\rangle = \frac{k^2 P\delta_1^5}{504}(1 + O(\delta_1)). \tag{34}$$

References

[1] M. E. Stern, *Ocean Circulation Physics*, *International Geophysics Series, vol 19* (Academic Press, New York, 1975).

[2] W. R. Young, Notes on Rossby's problem, 2002, private communication.

[3] A. Defant, *Physical Oceanography: Volume I* (MacMillan, New York, 1961).

[4] H. Jeffreys, "On fluid motions produced by differences of temperature and humidity," Quart. J. Roy. Meteorol. Soc. **51**, 347 (1925).

[5] T. Rossby, "On thermal convection driven by non-uniform heating from below: an experimental study," Deep-Sea Res. **12**, 9 (1965).

[6] R. C. Somerville, "A non-linear spectral model of convection in a fluid unevenly heated from below," J. Atmos. Sci. **24**, 665 (1967).

[7] R. C. Beardsley and J. F. Festa, "A numerical model of convection driven by surface stress and non-uniform horizontal heating," J. Phys. Ocean. **2**, 444 (1972).

[8] T. Rossby, "Numerical experiments with a fluid heated non-uniformly from below," Tellus **50A**, 242 (1998).

[9] F. Paparella and W. R. Young, "Horizontal convection is non-turbulent (preprint)," J. Fluid Mech. (2002).

[10] J. W. Sandström, "Dynamische Versuche mit Meerwasser," Annals in Hydrodynamic Marine Meteorology (1908).

[11] U. Frisch, *Turbulence: the legacy of A. N. Kolmogorov* (Camb. Univ. Press, Cambridge, 1995).

[12] C. R. Doering and P. Constantin, "Variational bounds on energy dissipation in incompressible flows. III. Convection," Phys. Rev. E **53**, 5957 (1996).

[13] M. H. Protter and H. F. Weinberger, *Maximum Principles in Differential Equations* (Springer–Verlag, New York, 1984).

[14] R. H. Kraichnan, "Turbulent thermal convection at arbitrary Prandtl number," Phys. Fluids **5**, 1374 (1962).

[15] E. A. Spiegel, "Convection in stars," Annu. Rev. Astron. Astr. **9**, 323 (1971).